Cluster size dependence of double ionization energy spectra of spin-polarized aluminum and sodium clusters: All-electron spin-polarized $GW+T$-matrix method

Yoshifumi Noguchi
Institute for Solid State Physics, The University of Tokyo, 5-1-5 Kashiwanoha, Kashiwa, Chiba 277-8581, Japan and Computational Materials Science Center, National Institute for Materials Science, 1-2-1 Sengen, Tsukuba, Ibaraki 305-0047, Japan

Kaoru Ohno
Department of Physics, Graduate School of Engineering, Yokohama National University, 79-5 Tokiwadai, Hodogaya, Yokohama 240-8501, Japan

Igor Solovyev and Taizo Sasaki
Computational Materials Science Center, National Institute for Materials Science, 1-2-1 Sengen, Tsukuba, Ibaraki 305-0047, Japan
(Received 7 December 2009; revised manuscript received 1 March 2010; published 7 April 2010)

The double ionization energy (DIE) spectra are calculated for the spin-polarized aluminum and sodium clusters by means of the all-electron spin-polarized $GW+T$-matrix method based on the many-body perturbation theory. Our method using the one- and two-particle Green's functions enables us to determine the whole spectra at once in a single calculation. The smaller is the size of the cluster, the larger the difference between the minimal double ionization energy and the twice of the ionization potential. This is because the strong Coulomb repulsion between two holes becomes dominant in small confined geometry. Due to Pauli's exclusion principle, the parallel spin DIE is close to or smaller than the antiparallel spin DIE except for Na_4 that has well-separated highest and second highest occupied molecular-orbital levels calculated by the spin-dependent GW calculation. In this paper, we compare the results calculated for aluminum and sodium clusters and discuss the spin-polarized effect and the cluster size dependence of the resulting spectra in detail.

DOI: 10.1103/PhysRevB.81.165411 PACS number(s): 73.22.−f, 71.15.Qe, 71.10.−w, 71.15.Ap

I. INTRODUCTION

The density-functional theory (DFT) together with its local-density approximation (LDA) or the generalized gradient approximation (GGA) has been very widely used in calculating the electronic states and atomic geometries of various materials including molecules, clusters, surfaces, and crystals.[1] In spite of its great success in determining the electronic ground-state properties, it has been also emphasized that DFT cannot directly determine the quasiparticle spectra of the electronic excited states because the auxiliary Kohn-Sham orbitals and eigenvalues do not represent the true quasiparticle wave functions nor the true quasiparticle energies. To determine the quasiparticle energy spectra correctly, it is necessary to go beyond the DFT.

The most popular method to determine the single quasiparticle energy spectra is the so-called GW approximation (GWA), in which the one-electron self-energy operator (Σ) is approximated as a product of a one-particle Green's function (G_1) and a dynamically screened Coulomb interaction (W) obtained within the random-phase approximation (RPA).[1–6] To calculate the double quasiparticle energy spectra, whose minimal value corresponds to the double ionization energy (DIE) or the double electron affinity (DEA), which are the sum of the first and second ionization potentials (IPs) or electron affinities (EAs), it is necessary to further calculate the (hole-hole or electron-electron) two-particle Green's function. A special care should be paid in calculating the two-particle Green's function in particular for small sized systems because the two holes (electrons) are confined in the small region and the Coulomb repulsion between them becomes strong. Therefore, the problem of the short-range electron correlations such as the Coulomb hole plays a very important role in determining the double quasiparticle states.

We have developed an all-electron $GW+T$-matrix code, which enables us to sum up particle-particle ladder diagrams up to the infinite order by solving the Bethe-Salpeter equation for the two-particle Green's function, and applied it to the calculation of DIE and DEA spectra[7] as well as the two-particle (double quasiparticle) wave functions of small molecules.[8] We have also extended it to the calculation of Auger spectra of hydrocarbon systems[9] and to the Hubbard U of 1,3,5–trithia-2,4,6–triazapentalenyl (TTTA) radical Mott insulator.[10]

Recently, quantum dots made of metal and semiconductor clusters have attracted much interest in a sense that their optical or conducting properties can be easily controlled by the size of the clusters.[5] Among them, spin-polarized clusters would provide further fascinating objects in the future spintronics applications. In these circumstances, it would be very important to accurately determine the spectroscopic properties of the spin-polarized clusters from reliable first-principles calculation beyond the framework of the DFT.

In the present study, using the spin-polarized $GW+T$-matrix theory, we have calculated the one- and two-particle (quasiparticle) energy spectra of the aluminum and sodium clusters with the size of up to eight atoms. Since the single quasiparticle energy spectra for the sodium clusters were reported in our previous paper,[6] here we show the result for the aluminum clusters. As for the double ionization quasiparticle energy spectra, we present the results of both aluminum and sodium clusters. We discuss the spin-polarization effects and the cluster size dependence of the resulting spectra in detail.

II. METHODOLOGY

The present excited-state calculations are performed by using the all-electron mixed basis approach in which a wave function is expanded as a linear combination of the numerical atomic orbitals (AOs) generated by Herman-Skillman's atomic code and the plane waves (PWs). By the use of PWs, the free-electron states above the vacuum level, which are required in an explicit treatment in perturbation theory because of the summation for empty states, are treated accurately. And also the AOs mainly contribute to the localized states such as the core electron states. Consequently, the whole states from localized to extended states are expressed efficiently with a relatively small basis set.

We use a supercell approximation due to the use of PWs in expanding the wave function. The fcc supercell we choose in the present calculation has a cubic edge of 31.9 Å. To eliminate the interaction with the clusters in the nearest-neighbor cells, we also use the spherical cut technique in which the long tail part of Coulomb interaction $1/r$ is abruptly cut at the half of the supercell size. The required PW cutoff energy is about 4.25 Ry, and the G vectors with 12.5 Ry in the evaluation of the Fock-exchange term and the G (G') vectors with 2.2 Ry in the evaluation of the correlation term are enough to achieve a good convergence within 0.1 eV. In addition, for the correlation term, we also need a few thousand valence levels corresponding to 25.2 eV.

A. *GW*+*T*-matrix formalism

First we introduce the spin-polarized *GW* (sp*GW*) formalism.[6] In the spin-polarized version of *GW*, the self-energy operator is simply expressed as $\Sigma_\sigma^{\mathrm{sp}GW}=iG_{1,\sigma}W$, where σ is the spin index. The expectation value of this self-energy operator is added to the local spin density aproximation (LSDA) Kohn-Sham orbital energy to determine the sp*GW* quasiparticle energy with the renormalization factor $Z_{\nu,\sigma}$,

$$E_{\nu,\sigma}^{\mathrm{sp}GW}=E_{\nu,\sigma}^{\mathrm{LSDA}}+Z_{\nu,\sigma}\langle\nu,\sigma|\Sigma_\sigma^{\mathrm{sp}GW}(E_{\nu,\sigma}^{\mathrm{LSDA}})-\mu_\sigma^{xc}|\nu,\sigma\rangle, \quad (1)$$

$$Z_{\nu,\sigma}=\frac{1}{1-\langle\nu,\sigma|\,\partial\Sigma_\sigma^{\mathrm{sp}GW}(E_{\nu,\sigma}^{\mathrm{LSDA}})/\partial E_{\nu,\sigma}^{\mathrm{LSDA}}|\nu,\sigma\rangle}, \quad (2)$$

where μ_σ^{xc} is the LSDA exchange-correlation potential. The present single quasiparticle calculations are all performed in a manner of *one-shot GW* formalism, namely, the LSDA Kohn-Sham orbital energies and the wave functions are used through the calculations. Recently, a problem of the LDA was pointed out in the *GW* calculation of the sodium clusters.[11]

Next, we expand the electron-electron (or hole-hole) two-particle Green's function into the ladder diagrams up to the infinite order (ladder approximation) as $G_2^T=G_2^0+G_2^0vG_2^0+G_2^0vG_2^0vG_2^0+\cdots$, where v is a bare Coulomb interaction and G_2^0 is a zeroth-order two-particle Green's function, which is given by a simple product of two one-particle Green's functions. The ladder part in G_2^T describing the multiple scattering between two particles is known as T matrix, which is connected with the G_2^T as follows:

$$\int d3'd4'T(1,2|3',4')G_2^0(3',4'|3,4)=v(1,2)G_2^T(1,2|3,4) \quad (3)$$

and the concrete form of T matrix is given in Eq. (4). Using the accurate quasiparticle energies obtained in the spGW calculation, we construct the spin-polarized T-matrix method. For these purposes, we work in matrix representation. Sandwiching all operators with the LSDA eigenstates (α, β, γ, and δ), we obtain the following matrix form for the Bethe-Salpeter equation:

$$T_{\sigma\sigma'}^{\alpha\beta\gamma\delta}(\omega)=v_{\sigma\sigma'}^{\alpha\beta\gamma\delta}+\sum_{\nu\mu}v_{\sigma\sigma'}^{\alpha\beta\nu\mu}G_{2,\sigma\sigma'}^{0,\nu\mu}(\omega)T_{\sigma\sigma'}^{\nu\mu\gamma\delta}(\omega), \quad (4)$$

where $G_{2,\sigma\sigma'}^0=iG_{1,\sigma}^{GW}G_{1,\sigma'}^{GW}$. For the spin unpolarized systems, all spin indices $\sigma(\sigma')$ disappear. After introducing an ω-independent two-particle Hamiltonian

$$H_{\sigma\sigma'}^{\alpha\beta\nu\mu}\equiv\left(\frac{f_{\nu\mu}}{G_{2,\sigma\sigma'}^{0,\nu\mu}(\omega)}-\omega\right)\delta_{\alpha\nu}\delta_{\beta\mu}-v_{\sigma\sigma'}^{\alpha\beta\nu\mu}f_{\nu\mu}$$
$$=\sum_{\nu\mu}(-E_{\nu,\sigma}^{\mathrm{sp}GW}-E_{\mu,\sigma'}^{\mathrm{sp}GW})f_{\nu\mu}\delta_{\alpha\nu}\delta_{\beta\mu}-v_{\sigma\sigma'}^{\alpha\beta\nu\mu}f_{\nu\mu}, \quad (5)$$

Eq. (4) can be rearranged into more convenient form

$$f_{\alpha\beta}G_{2,\sigma\sigma'}^{0,\alpha\beta}(\omega)T_{\sigma\sigma'}^{\alpha\beta\gamma\delta}(\omega)=\sum_{\nu\mu}(H_{\sigma\sigma'}^{\alpha\beta\nu\mu}+\omega)^{-1}v_{\sigma\sigma'}^{\nu\mu\gamma\delta}, \quad (6)$$

where $f_{\nu\mu}=-\delta_\nu^{occ}\delta_\mu^{occ}+\delta_\nu^{emp}\delta_\mu^{emp}$. In other words, by obtaining the two-particle Green's function as $G_2^T(\omega)=(H+\omega)^{-1}$, we recover the standard definition for the T-matrix [see Eq. (3)]. In this formalism, therefore, the poles of the two-particle Green's function are obtained as the eigenvalues $\Omega_{i,\sigma\sigma'}$ of the eigenvalue problem

$$\sum_{\nu\mu}H_{\sigma\sigma'}^{\alpha\beta\nu\mu}A_{i,\sigma\sigma'}^{\nu\mu}=\Omega_{i,\sigma\sigma'}A_{i,\sigma\sigma'}^{\alpha\beta}. \quad (7)$$

The two-particle wave functions,

$$\Psi_{i,\sigma\sigma'}(\boldsymbol{r}_1,\boldsymbol{r}_2)=\sum_{\nu\mu}A_{i,\sigma\sigma'}^{*,\nu\mu}\psi_{\nu,\sigma}(\boldsymbol{r}_1)\psi_{\mu,\sigma'}(\boldsymbol{r}_2), \quad (8)$$

given by solving the Bethe-Salpeter equation can be either symmetric or antisymmetric with respect to the interchange of the particles. For spin-unpolarized systems, the former is identified to be the singlet state because antisymmetric spin part must be multiplied and the latter is identified to be the triplet state because symmetric spin part must be multiplied. Since no spin polarization exists at the outset, we know that the spin multiplicity of the two-particle states directly corresponds to the spin multiplicity of the resulting double ionized, $(N\pm2)$-particle excited states.

B. Spin multiplicity and antisymmetrization

For spin-polarized systems, the ground states are degenerate according to the spin multiplicity (note that, even for these systems, it is not necessary to adopt perturbation theory for degenerate states because off-diagonal blocks of the T matrix bridging between different ground states do not exist).

As well as spin unpolarized systems, the double ionized, $(N\pm 2)$-particle excited states are created by removing or adding two electrons from any one of the ground states, and the spin multiplicity of the resulting excited states must be identified. However, in the present description of the quantum states based on the spin-dependent one-particle states, we consider only the maximally polarized spin states, i.e., the states with $S_z=\pm S$, where S is the total spin of the system, although, in principle, it might be possible to consider the other states such that $S_z\neq\pm S$ by rotating the whole system by arbitrary angles. Therefore, for example, if we remove two electrons with parallel $\uparrow\uparrow$ $(\downarrow\downarrow)$ spins from the systems, the spin state of the resulting $(N-2)$-electron system has $S'=S_z-1$ and $S'_z=|S_z-1|$ (or $S'_z=S_z+1$ and $S'_z=|S_z+1|$). Or, if we remove two electrons with antiparallel $\uparrow\downarrow$ spins from the system, the spin state of the resulting $(N-2)$-electron system is unchanged, i.e., $S'_z=S_z$ and $S'=S$. The other $(N-2)$-electron excited states might be considered by rotating the whole system by arbitrary angles, but, unfortunately, we do not know at the moment how to describe it within the present mathematical formalism allowing just maximally polarized spin states. This problem is, however, beyond the scope of the present paper and is left for the future study.

For spin-polarized systems, therefore, we have only three cases to consider when we remove two electrons: $\uparrow\uparrow$, $\downarrow\downarrow$, and $\uparrow\downarrow$. These spin arrows correspond to the indices appearing in Eqs. (4)–(8). In the two-particle states (8), given by solving the corresponding Bethe-Salpeter equation, only antisymmetric solutions are allowed because of the Pauli principle for the two-particle states.

C. ↑↑ and ↓↓ two-hole states

Let us look more explicitly at the structure of the Hamiltonian (5). First, suppose a $\uparrow\uparrow$ two-particle state made of both left and right particles having a majority spin, $(\uparrow)$. In this paper, we express the two-hole state as $n_{\nu\sigma}$ $(m_{\mu\sigma'})$, where $n_{\nu\sigma}$ $(m_{\mu\sigma'})$ denotes one hole state with σ (σ') spin at ν (μ)th level, and symbolize for simplicity the each matrix element constituting the two-particle Hamiltonian [Eq. (5)] as $A,B,C,D,\alpha,\beta,\delta,\gamma$, etc. Then the Hamiltonian for the two-particle state $\uparrow\uparrow$ in the matrix form of the Bethe-Salpeter equation may be written as

$$\begin{array}{c} \\ n_{1\uparrow}n_{2\uparrow} \\ n_{1\uparrow}n_{3\uparrow} \\ \vdots \\ n_{2\uparrow}n_{1\uparrow} \\ n_{3\uparrow}n_{1\uparrow} \\ \vdots \end{array} \begin{array}{c} \begin{array}{cccccc} n_{1\uparrow}n_{2\uparrow} & n_{1\uparrow}n_{3\uparrow} & \cdots & n_{2\uparrow}n_{1\uparrow} & n_{3\uparrow}n_{1\uparrow} & \cdots \end{array} \\ \begin{pmatrix} A & \Delta & \cdots & \alpha & \delta & \cdots \\ \Delta^* & B & \cdots & \beta & \gamma & \cdots \\ \vdots & \vdots & \ddots & \vdots & \vdots & \cdots \\ \alpha^* & \beta^* & \cdots & C & \eta & \cdots \\ \delta^* & \gamma^* & \cdots & \eta^* & D & \cdots \\ \vdots & \vdots & \cdots & \vdots & \vdots & \cdots \end{pmatrix} \end{array}. \tag{9}$$

Here, we have to keep the index $n_{\nu\uparrow}n_{\mu\uparrow}$ as well as the index $n_{\mu\uparrow}n_{\nu\uparrow}$ because we want to antisymmetrize the resulting two-particle wave function. This matrix (9) does not have components such as

$$n_{1\uparrow}n_{1\uparrow} \quad n_{2\uparrow}n_{2\uparrow} \quad \cdots \quad n_{n\uparrow}n_{n\uparrow} \quad n_{n+1\uparrow}n_{n+1\uparrow} \quad \cdots . \tag{10}$$

What we should do is to diagonalize Eq. (9), extract only the solutions that are antisymmetrized with respect to $n_{1\uparrow}n_{1\uparrow}$ and $n_{2\uparrow}n_{2\uparrow}$, and simply discard their symmetrized counterparts, which are not allowed due to the Pauli principle.

The case where we remove $\downarrow\downarrow$ electrons can be treated in the same way as this case by just inverting all the spin directions. We do not repeat the explanation for redundancy.

D. ↑↓ and ↓↑ two-hole states

Next, let us suppose a $\uparrow\downarrow$ two-particle state made of left particle having a majority spin, $(\uparrow)$, and right particle having a minority spin, $(\downarrow)$. Then the Hamiltonian for the two-particle state $\uparrow\downarrow$ in the matrix eigenvalue form of the Bethe-Salpeter equation (5) may be written as

$$\begin{array}{c} \\ n_{1\uparrow}m_{1\downarrow} \\ n_{1\uparrow}m_{2\downarrow} \\ \vdots \\ n_{2\uparrow}m_{1\downarrow} \\ n_{2\uparrow}m_{2\downarrow} \\ \vdots \end{array} \begin{array}{c} \begin{array}{cccccc} n_{1\uparrow}m_{1\downarrow} & n_{1\uparrow}m_{2\downarrow} & \cdots & n_{2\uparrow}m_{1\downarrow} & n_{2\uparrow}m_{2\downarrow} & \cdots \end{array} \\ \begin{pmatrix} A & \Delta & \cdots & \alpha & \beta & \cdots \\ \Delta^* & B & \cdots & \gamma & \epsilon & \cdots \\ \vdots & \vdots & \ddots & \vdots & \vdots & \cdots \\ \alpha^* & \gamma^* & \cdots & C & \delta & \cdots \\ \beta^* & \epsilon^* & \cdots & \delta^* & D & \cdots \\ \vdots & \vdots & \cdots & \vdots & \vdots & \cdots \end{pmatrix} \end{array}. \tag{11}$$

If we diagonalize this Hamiltonian matrix, the resulting eigenfunctions are not symmetrized with respect to the interchange of the particles.

Similarly, we could consider a two-particle state with $\downarrow\uparrow$ spin, supposing that left particle has a minority spin, $(\downarrow)$, and the right particle has a majority spin, $(\uparrow)$. In this case, the Hamiltonian for the two-particle state $\downarrow\uparrow$ is given by

$$\begin{array}{c} \\ m_{1\downarrow}n_{1\uparrow} \\ m_{2\downarrow}n_{1\uparrow} \\ \vdots \\ m_{1\downarrow}n_{2\uparrow} \\ m_{2\downarrow}n_{2\uparrow} \\ \vdots \end{array} \begin{array}{c} \begin{array}{cccccc} m_{1\downarrow}n_{1\uparrow} & m_{2\downarrow}n_{1\uparrow} & \cdots & m_{1\downarrow}n_{2\uparrow} & m_{2\downarrow}n_{2\uparrow} & \cdots \end{array} \\ \begin{pmatrix} A & \Delta & \cdots & \alpha & \beta & \cdots \\ \Delta^* & B & \cdots & \gamma & \epsilon & \cdots \\ \vdots & \vdots & \ddots & \vdots & \vdots & \cdots \\ \alpha^* & \gamma^* & \cdots & C & \delta & \cdots \\ \beta^* & \epsilon^* & \cdots & \delta^* & D & \cdots \\ \vdots & \vdots & \cdots & \vdots & \vdots & \cdots \end{pmatrix} \end{array}. \tag{12}$$

The eigenvalues and eigenfunctions of Eq. (12) coincide with those of Eq. (11) except that the order of left and right (level, spin) indices are inverted in the eigenfunctions. Then, if we introduce the double Hamiltonian matrix having a block-diagonal form of Eqs. (11) and (12), the resulting eigenvalues are the same as those of Eqs. (11) and (12) and the resulting eigenfunctions are either symmetric or antisymmetric with respect to the two-particle states, $n_{i\uparrow}m_{j\downarrow}$ and $m_{j\downarrow}n_{i\uparrow}$; the symmetrized and antisymmetrized solutions are degenerate because of the absence of the off-diagonal block bridging between two-particle states $(n_{i\uparrow}m_{j\downarrow})$ and $(m_{k\downarrow}n_{l\uparrow})$ in the double Hamiltonian.

In our description, a one-particle wave function contains spin part in it, i.e., we have only up-spin spatial wave func-

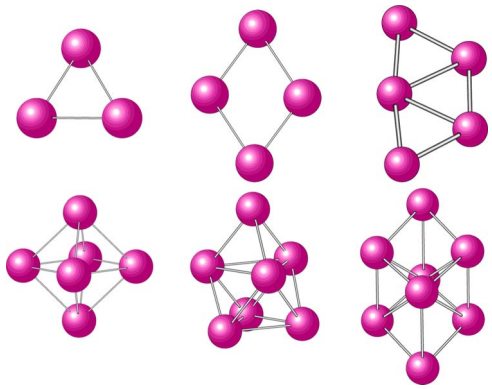

FIG. 1. (Color online) Most stable geometry of Al_n ($n=1-8$) clusters. The smallest bond length in each cluster is listed in Table I.

tions and down-spin spatial wave functions. Since the two-particle wave functions are made of these one-particle wave functions, only antisymmetrized counterparts of the two-particle wave functions are allowed. Therefore, we can simply discard the symmetrized counterpart of the two-particle wave functions. As a result, the eigenvalues obtained by diagonalizing the double Hamiltonian matrix are exactly the same as the eigenvalues obtained by diagonalizing just either Eq. (9) or (11).

III. RESULTS AND DISCUSSIONS

A. Atomic geometries and magnetic moments

First, we performed the atomic geometry optimization by using the GAUSSIAN 03 program package[12] within GGA proposed by Becke, Perdew, and Wang (BPW91) (Refs. 13 and 14) and a large basis set (6-311G*).[15] In this calculation, all molecular orbitals from core to valence ones were fully optimized. Prior to this work, Rao and Jena[16] already performed similar geometry optimization with the GGA and the frozen-core approximation for the aluminum $1s$, $2s$, and $2p$ states. Since they discussed the stability and structure of aluminum clusters in many details, their work was used as a guidance in our study. Indeed, the resulting optimized structures obtained in our work are almost the same as in the work of Rao and Jena.[16] Figure 1 shows the most stable atomic geometries optimized for the neutral aluminum clusters (Al_n, $n=3-8$). The geometries of the Al_n clusters are planer structures for $n \leq 5$ and three-dimensional structures for $n \geq 6$. This tendency is similar to the one seen in other metal clusters such as the lithium, sodium, and potassium clusters, although the bond lengths and symmetries are a little different.[5,6]

The nearest-neighbor distance between aluminum atoms and the magnetic moment of aluminum clusters for the neutral ground state are listed in Table I. The significant difference with the alkali-metal clusters is that the high spin state of Al_n is stable for $n=2$, 4, and 6 despite the fact that the system has even number of electrons.

B. Single quasiparticle energy spectra

Figure 2 shows the sp*GW* quasiparticle energy spectra of aluminum clusters together with the LSDA Kohn-Sham orbital energy spectra for comparison. Only the valence levels and some unoccupied levels located below the vacuum level at 0 eV are shown. In this figure, the experimental IP (Refs. 17 and 18) and EA (Ref. 19) with negative signs are indicated by the horizontal arrows and the highest hole (highest occupied molecular orbital, HOMO) and lowest electron (lowest unoccupied molecular orbital, LUMO) levels correspond to these arrows indicated by IP and EA, respectively.

TABLE I. Nearest-neighbor distance between Al atoms and the magnetic moment calculated for the neutral aluminum clusters.

	Nearest-neighbor distance (Å)	Magnetic moment (μ_B)
Al_1		1
Al_2	2.77	2
Al_3	2.53	1
Al_4	2.57	2
Al_5	2.49	1
Al_6	2.56	2
Al_7	2.60	1
Al_8	2.56	0

For an isolated aluminum atom in which one $3p$ level is occupied by an $\uparrow$ spin electron, the LSDA $\uparrow$ spin and $\downarrow$ spin $3p$ levels are both triply degenerate, while the *GW* $3p$ quasiparticle energies split into singly and doubly degenerate levels, forming the energy gap; the lowest $\uparrow$ spin level is the single hole (occupied) level and the rest are electron (empty) levels. For an aluminum dimer, the ground state is spin triplet. Within the LSDA, a single σ_g (bonding p orbitals parallel to the dimer axis) and the doubly degenerate π_u (bonding p orbitals perpendicular to the dimer axis) levels are almost degenerate and two of these three levels (the σ_g and one of the π_u levels) are occupied by $\uparrow$ spin electrons. In contrast, in the *GW* quasiparticle energy spectra, the $\uparrow$ spin σ_g level and one of the $\uparrow$ spin π_u levels are still almost degenerate, forming the hole (occupied) levels, and the other $\uparrow$ spin π_u level is split off from the originally doubly degenerate, forming the energy gap.

Here we must mention the treatment of *divergence* of the polarization function in calculating the *GW* correlation term for aluminum atom and dimer of which HOMO and LUMO are degenerated at the ground state. Although the denominator of the polarization function becomes zero at the transition from HOMO to LUMO, the corresponding numerator is also zero for the degenerate states. Therefore, the HOMO-LUMO transitions such as $3p \rightarrow 3p$ for aluminum atom and $\pi \rightarrow \pi$ for aluminum dimer are forbidden and do not contribute to the *GW* correlation energy.

As well known, the LSDA Kohn-Sham orbital energy spectra are quite different from the sp*GW* quasiparticle energy spectra. The *GW* hole (occupied) and electron (unoccupied) levels are, respectively, deeper and shallower by a few electron volts than the LSDA and consequently the LSDA HOMO-LUMO gap is greatly improved. Also the LSDA eigenvalues at LUMO level are too deep compared to the arrow indicated as EA (the difference is about 1.3–2.5 eV).

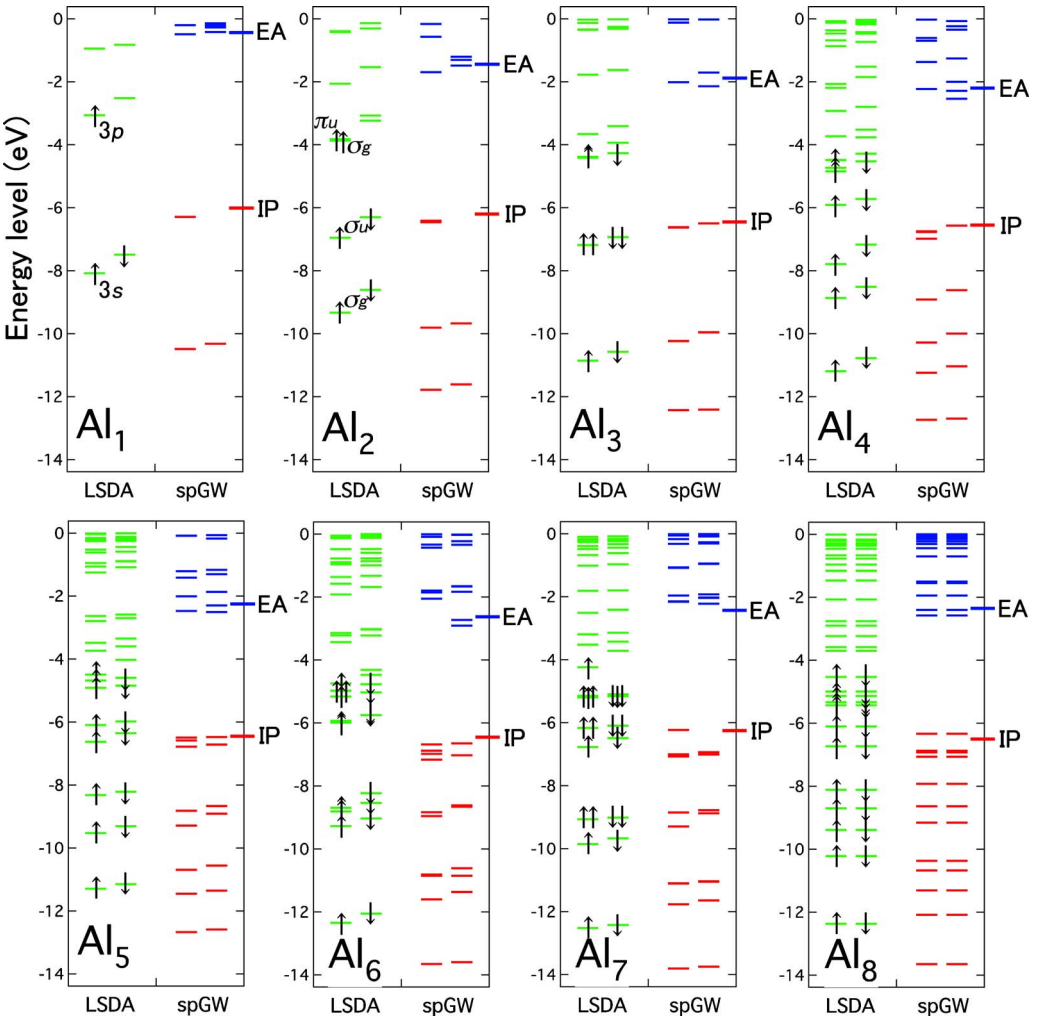

FIG. 2. (Color online) Calculated sp*GW* quasiparticle energy spectra including all valence hole (occupied) levels and a few conduction-electron (unoccupied) levels below the vacuum level (0 eV). Also corresponding LSDA Kohn-Sham orbital energies are listed for comparison. Vertical arrows denote the spin directions of the occupied electrons. The experimental ionization potentials (Refs. 17 and 18) and electron affinities (Ref. 19) with negative signs are indicated as IP and EA, respectively.

HOMO-LUMO gap estimated by the LSDA is zero for Al_1 and Al_2 (due to the twofold-degenerate HOMO ↑ and LUMO ↑ levels), although the experimental gap is about 3.8–5.5 eV (note that there is no significant improvement to the difference between the Kohn-Sham orbital energy and the experiment if the exchange-correlation functional is replaced by the GGA). Nevertheless, the overall cluster size dependence of IP and EA has a similar tendency to the LSDA eigenvalues. That is, HOMO level energy (corresponding to IP with negative sign) almost does not change as the cluster size. The only exception is the Al_6 cluster, where LUMO level energy (corresponding to EA with negative sign) is slightly deeper compared to that of Al_7. This irregular behavior may be attributed to the shape of the clusters. Al_n ($n \leq 5$) have planer structures, while larger clusters have three-dimensional structures and Al_6 has a compact three-dimensional structure.

For small-sized clusters up to the trimer, the hole (occupied) levels are energetically well separated from each other due to their small number of valence levels. Therefore, the comparison between the LSDA and sp*GW* spectra is easy and the change from the LSDA to the sp*GW* looks like almost constant shift. On the other hand, the situation becomes a little complicated for larger sized clusters because the density of valence levels increases. In addition, although the basic tendency that the sp*GW* expands the small LSDA gap is the same, there is a significant difference between the LSDA and the sp*GW* when we compare the relative position of the highest hole (occupied) levels with the ↑ and ↓ spin in particular for Al_{4-6}. In the LSDA, the highest hole level with ↓ spin is lower than that with the ↑ spin and vice versa in the sp*GW*. This difference becomes significant when we consider the cationic ground state where one electron is removed from the highest occupied level. The LSDA predicts lower spin state in cations than the neutral clusters, while the sp*GW* predicts the higher spin state in cations than the neutral clusters.

In order to confirm the present result, we have also performed the total-energy calculation by using the GAUSSIAN 03 program package. Table II lists the resulting magnetic moment (in μ_B) of aluminum clusters at neutral, cationic, and anionic states with the same geometry. The change in the geometry is small and negligible in the charged states of the

TABLE II. Magnetic moment (μ_B) of aluminum clusters at the neutral, cation, and anion.

	LSDA			GGA		
	Neutral	Cation	Anion	Neutral	Cation	Anion
Al_1	1	0	2	1	0	2
Al_2	2	1	3	2	1	3
Al_3	1	2	0	1	2	0
Al_4	2	1	1	2	3	1
Al_5	1	0	0	1	2	0
Al_6	2	1	1	2	3	1
Al_7	1	0	0	1	0	0
Al_8	0	1	1	0	1	1

aluminum (and sodium clusters). From this table, we find that the LSDA spin configuration of cations speculated from Fig. 2 is fully consistent with the corresponding magnetic moment of LSDA (total-energy) ground states of cations. Our sp*GW* result is not consistent with the magnetic moment of the LSDA ground state of cations. Our sp*GW* result is consistent with the magnetic moment of the GGA (total-energy) ground state of cations.

IP and EA calculated by the total-energy difference between the N-electron system and $N-1$ $(N+1)$-electron ionized system are listed in Table III together with our sp*GW* results and the available experimental data. The LSDA and GGA total-energy difference, known as delta self-consistent field (ΔSCF) method, can estimate the IP and EA reasonably well [note that, although ΔSCF (LSDA) has a little discrepancy with the experiment, an overestimation of about 0.4–1.1 eV for IP and 0.0–0.5 eV for EA, ΔSCF (GGA) agrees with the experiment relatively well in particular for small-sized clusters]. The agreement of the sp*GW* quasiparticle energies with the experimental values is also fairly good. The remaining error of the sp*GW* is only about 0.0–0.3 eV for IP and EA.

C. Double ionization energies

By using the one-particle Green's function determined by the sp*GW* calculation, we now proceed to the calculation of DIE spectra of aluminum and sodium clusters. The keypoint in this calculation is the short-range repulsive Coulomb interaction (or the so-called multiple scattering) between two holes. This kind of interaction, which is described properly by neither simple bare Coulomb interaction expressed by $1/r$ nor the dynamically screened Coulomb interaction such as used in the GWA, requires the treatment of the hole-hole ladder diagrams up to the infinite order (T-matrix theory). The eigenvalues in Eq. (7) include the effect of the short-range electron correlations because they are equal to the poles of the hole-hole two-particle Green's function associated with the T matrix. Therefore, the present method has a potential to give a reliable estimate of the DIE spectra of the aluminum and sodium clusters.

To our knowledge, there is unfortunately no experimental data of DIE of aluminum and sodium clusters ($n \geq 2$). Nevertheless, to check the accuracy of the present result, we can compare the DIE calculated for an aluminum atom to the experiment.[20] The ground state of aluminum atom is spin doublet with total spin $S=1/2$. If we remove one $\uparrow$ electron and one $\downarrow$ electron simultaneously from either one of the doublet ground states, the resulting state becomes also doublet. In this case, from Eq. (9), we obtain $\Omega_{\uparrow\downarrow}=24.8$ eV for the DIE. On the other hand, if we remove two $\uparrow$ electrons

TABLE III. Calculated first IPs and EAs of aluminum clusters (in eV) together with the experimental values [IP (Refs. 17 and 18), EA (Ref. 19)]. The ΔSCF calculations are performed by GAUSSIAN 03 program package.

		ΔSCF (LSDA)	ΔSCF (GGA)	sp*GW*	Expt.
Al_1	IP	6.45	6.08	6.29	6.00 ± 0.12
	EA	0.95	0.49	0.49	0.44 ± 0.01
Al_2	IP	6.81	6.26	6.41	6.20 ± 0.20
	EA	2.01	1.47	1.69	1.46 ± 0.06
Al_3	IP	7.25	6.56	6.50	6.45 ± 0.05
	EA	2.31	1.71	2.14	1.89 ± 0.04
Al_4	IP	7.28	6.60	6.57	6.55 ± 0.05
	EA	2.64	2.06	2.54	2.20 ± 0.05
Al_5	IP	7.13	6.59	6.47	6.45 ± 0.05
	EA	2.62	2.02	2.50	2.25 ± 0.05
Al_6	IP	7.47	6.81	6.64	6.45 ± 0.05
	EA	3.01	2.38	2.91	2.63 ± 0.06
Al_7	IP	6.79	6.27	6.23	6.25 ± 0.20
	EA	2.42	1.80	2.22	2.43 ± 0.06
Al_8	IP	6.94	6.42	6.33	6.50 ± 0.05
	EA	2.36	1.95	2.58	2.35 ± 0.08

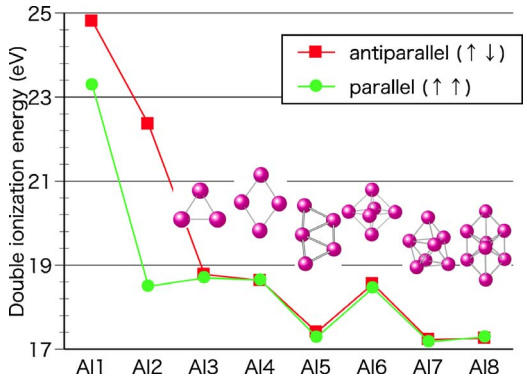

FIG. 3. (Color online) Cluster size dependence of DIE spectra of aluminum clusters. Squares and circles denote DIEs corresponding to the antiparallel and parallel spin states, respectively.

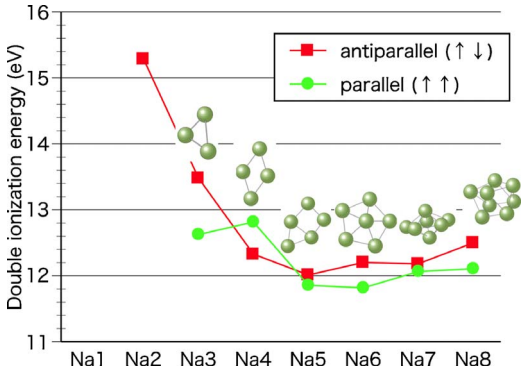

FIG. 4. (Color online) Cluster size dependence of DIE spectra of sodium clusters. Squares and circles denote DIEs corresponding to the antiparallel and parallel spin states, respectively.

from the $S_z=1/2(\uparrow)$ ground state, the result becomes also doublet. In this case, from Eq. (8), we obtain $\Omega_{\uparrow\uparrow}=23.3$ eV for the DIE. It is further possible to remove two $\downarrow$ electrons from the $S_z=1/2(\uparrow)$ ground state to obtain the $S_z=3/2$ excited state. Comparing these energies to the experimental DIE of 24.8 eV, we find that fairly good agreement is obtained for the theoretical result of the doublet final state. DIE is quite larger than the twice of IP because of the huge Coulomb repulsion between two holes created in the valence levels. In the aluminum atom case, the twice of IP is just 12.6 eV and too small compared to the experimental DIE of 24.8 eV.[17]

The ground state of aluminum dimer is spin triplet with total spin $S=1$. If we remove one $\uparrow$ electron and one $\downarrow$ electron simultaneously from either one of the two triplet ground states with $S_z=\pm 1$, the resulting state becomes either one of the two triplet excited states with $S_z=\pm 1$. Similarly, if we remove one $\uparrow$ electron and one $\downarrow$ electron simultaneously from the $S_z=0$ ground state, the resulting state split into the other one of the triplet excited states with $S_z=0$ and the $S=0$ singlet excited state. For getting either one of the triplet ground states, we obtain $\Omega_{\uparrow\downarrow}=22.4$ eV for the DIE from Eq. (9). On the other hand, if we remove two $\uparrow$ electrons from the $S_z=1$ ground state or two $\downarrow$ electrons from the $S_z=-1$ ground state, the resulting state becomes the same $S=0$ singlet excited state $S_z=0$. In this case, we obtain $\Omega_{\uparrow\uparrow}=18.5$ eV for the DIE from Eq. (8). It is further possible to remove two $\downarrow$ electrons from the $S_z=1$ ($\uparrow\uparrow$) ground state to obtain the $S=2$ excited state. In this case, also from Eq. (8), we obtain $\Omega_{\downarrow\downarrow}=26.4$ eV for the DIE.

Figure 3 shows the cluster size dependence of the DIE for the parallel and antiparallel spin states of aluminum clusters. As a general tendency, the DIE gradually decreases as the cluster size increases. This can be interpreted as: the two holes getting enough space to avoid each other as the cluster size increases, then the repulsive Coulomb interaction consequently becoming weaker. However, there is an irregular behavior at Al_6. This anomaly in the size dependence in the DIE may be related to the fact that Al_n ($n \leq 5$) have planar structures and larger clusters have three-dimensional structures. That is, the space where two holes can avoid each other must be somewhat more restricted at the compact structure of Al_6. Thus we observe here the strong cluster geometry (or size) dependence in the DIE. On the other hand, the spin configuration of the lowest DIE state seems to be determined by the repulsive Coulomb interaction between holes. As shown in Fig. 3, the parallel spin DIE has a nearly same or slightly smaller value than the antiparallel spin DIE, nevertheless, the summation of the two single-quasiparticle energies at the highest occupied levels with antiparallel spin configuration is shallower (i.e., energetically more favorable) than parallel spin configuration (aluminum atom and dimer are exceptional because of the degenerate or very close HOMO and HOMO−1 levels). This is because of the weaker short-range repulsive Coulomb interaction between parallel spin electrons. As it follows from the discussion of the radial distribution function for electron-gas systems, the parallel spin holes cannot come close to each other (exchange hole) due to the limitation of the short distance in Pauli's exclusion principle. On the other hand, the antiparallel spin holes can come close to each other because of the lack of Pauli's exclusion principle, although the population of these states decreases due to the Coulomb repulsion (Coulomb hole). The difference between the exchange hole and the Coulomb hole leads to the tendency that the Coulomb interaction exerts weakly between parallel spin holes and strongly between antiparallel spin holes, and consequently we have the small parallel DIE and the large antiparallel DIE. This preference is significant in determining the DIE and the spin configuration at the lowest DIE and dominates the other factors such as the position of the single quasiparticle energies and the existence of the spin polarization.

Next in Fig. 4, we present DIEs of sodium clusters for comparison.[20] First, we notice that DIEs of sodium clusters are about ~6 eV smaller than those of aluminum clusters. The small DIE may be attributed to the long bond length at the ground-state geometry (for example, the bond length is about 3.21 Å at sodium dimer and 2.77 Å at aluminum dimer) and the large screening effect due to the larger cluster size and therefore larger polarizability of sodium clusters. Also in the case of sodium clusters, the short-range repulsive Coulomb interaction is the most important factor determining the spin configuration at the lowest DIE. However, we also observe the irregularities in Fig. 4. Since Na_4 has well-separated HOMO and HOMO−1 levels, the short-range repulsive Coulomb interaction between two holes is not strong

enough to reverse the order of the antiparallel and parallel DIEs. On the other hand, a deviation between the parallel and antiparallel spin DIEs at Na_6 and Na_8 is larger than that of Al clusters and show the difference in the behavior of the short-range electron correlations between two spin configurations. This result came from solving the two-particle Hamiltonian [Eq. (5)]. [Note that the HOMO level at Na_6 is degenerate and the HOMO and HOMO−1 levels at Na_8 are very close, namely, the DIEs for these degenerated (close) levels are estimated to be almost same value in the single-particle theory.] We mention in Sec. III B that the DIE slightly increases from Na_6 to Na_8 because of the more compact structure. Although we did not calculate the DIE for larger clusters in this study, we expect that the DIE decreases for larger clusters because there is enough space where two holes can avoid each other.

IV. SUMMARY

In this paper, we have developed the spin-polarized *GW* + *T*-matrix method on the basis of the all-electron mixed basis approach, in which one-particle wave function is expressed in a linear combination of both plane waves and atomic orbitals. The method begins with the LSDA calculation, which is used as the starting point for the sp*GW* calculation. Finally, the Bethe-Salpeter equation for the spin-dependent *T* matrix which is related to the two-particle Green's function is solved by the matrix diagonalization technique. One merit of this method is that the whole spin-dependent spectra are obtained just in a single calculation with rather high accuracy. We applied this method to the calculation of the single and double quasiparticle energy spectra of aluminum clusters and the sodium clusters. The resulting minimal sp*GW* quasiparticle energies agree fairly well with the experimental IP and EA with remaining error of 0.0–0.3 eV for IP and EA. The obtained DIE spectra have strong size dependence, indicating the strong Coulomb interaction. Here, we have clarified that the effect of the electron-electron Coulomb interaction and the multiple scattering between electrons become quite strong in particular in small-size clusters. Moreover, since the cations as well as the neutral clusters of aluminum favor high spin configuration, the cluster-size dependence of IP, EA, and DIE does not simply correspond to those expected from the simple LSDA eigenvalues. In addition, although the summation of the two single-quasiparticle energies of the highest occupied is shallower for antiparallel spins than parallel spins except for Al_2, the parallel-spin DIE is close to or smaller than the antiparallel-spin DIE due to the strong effect of Pauli's exclusion principle. The only exception is Na_4 that has well-separated HOMO and HOMO−1 levels calculated by the spin-dependent *GW* calculation. Also, the effect of spin polarization plays an important role in the resulting DIE spectra. Thus we confirm that the strong size dependence exists in the resulting DIE. We find a small even-odd oscillation in DIE spectra of sodium clusters. In the dependence of the resulting EA and DIE on the cluster size, the behavior of Al_6 is anyhow irregular, reflecting the fact that the structures of Al_n, with $n=1-5$, are planer, those with $n \geq 6$ are three dimensional, and Al_6 has a compact octahedral structure. All these results suggest the validity of the present method and the possibility in the future applications to other spin-polarized systems.

ACKNOWLEDGMENTS

The authors thank the National Institute for Materials Science and the Information Initiative Center, Hokkaido University, for the use of the Numerical Materials Simulator and the HITACHI SR11000 supercomputing facilities. The present work is partially supported by the Grant-in-Aid in Scientific Research on Priority Area (Grant No. 19019005) from the Ministry of Education, Culture, Sports, Science and Technology (MEXT) and also by the Grant-in-Aid in Scientific Research B (Grant No. 21340115) from the Japan Society of the Promotion of Science (JSPS).

[1] K. Ohno, K. Esfarjani, and Y. Kawazoe, *Introduction to Computational Materials Science—From Ab Initio to Monte Carlo Methods*, Springer Series on Solid-State Sciences Vol. 129 (Springer-Verlag, Berlin, 1999), and references therein.
[2] L. Hedin, Phys. Rev. **139**, A796 (1965).
[3] M. S. Hybertsen and S. G. Louie, Phys. Rev. B **34**, 5390 (1986).
[4] R. W. Godby, M. Schlüter, and L. J. Sham, Phys. Rev. B **37**, 10159 (1988).
[5] K. Ohno, M. Tanaka, J. Takeda, and Y. Kawazoe, *Nano- and Micromaterials*, Springer Series on Advances in Materials Research Vol. 9 (Springer-Verlag, Berlin, 2008), and references therein.
[6] Y. Noguchi, S. Ishii, K. Ohno, and T. Sasaki, J. Chem. Phys. **129**, 104104 (2008).
[7] Y. Noguchi, Y. Kudo, S. Ishii, and K. Ohno, J. Chem. Phys. **123**, 144112 (2005).
[8] Y. Noguchi, S. Ishii, and K. Ohno, J. Chem. Phys. **125**, 114108 (2006).
[9] Y. Noguchi, S. Ishii, K. Ohno, I. Solovyev, and T. Sasaki, Phys. Rev. B **77**, 035132 (2008).
[10] K. Ohno, Y. Noguchi, T. Yokoi, S. Ishii, J. Takeda, and M. Furuya, ChemPhysChem **7**, 1820 (2006).
[11] F. Bruneval, Phys. Rev. Lett. **103**, 176403 (2009).
[12] M. J. Frisch *et al.*, GAUSSIAN 03, Revision B.04, Gaussian, Inc., Wallingford, CT, 2004.
[13] A. D. Becke, Phys. Rev. A **38**, 3098 (1988).
[14] K. Burke, J. P. Perdew, and Y. Wang, in *Electronic Density Functional Theory: Recent Progress and New Directions*, edited by J. F. Dobson, G. Vignale, and M. P. Das (Plenum, New York, 1998).
[15] A. D. McLean and G. S. Chandler, J. Chem. Phys. **72**, 5639 (1980).
[16] B. K. Rao and P. Jena, J. Chem. Phys. **111**, 1890 (1999).
[17] C. Kittel, *Introduction to Solid State Physics*, 7th ed. (Wiley,

New York, 1995).
[18] K. E. Schriver, J. L. Persson, E. C. Honea, and R. L. Whetten, Phys. Rev. Lett. **64**, 2539 (1990).
[19] X. Li, H. Wu, X. B. Wang, and L. S. Wang, Phys. Rev. Lett. **81**, 1909 (1998).
[20] DIE of sodium atom involves the energy of core states and is not calculated in this paper. For the same reason, parallel DIE of sodium dimer is not calculated either.